JOURNAL OF GUIDANCE, CONTROL, AND DYNAMICS
Vol. 29, No. 4, July–August 2006

Unmanned Aerial Vehicle Dynamic-Target Pursuit by Using Probabilistic Threat Exposure Map

Atilla Dogan* and Ugur Zengin†
University of Texas at Arlington, Arlington, Texas 76019

A strategy is presented for an unmanned aerial vehicle (UAV) to follow a moving target in an area the probabilistic threat exposure map of which is assumed to be known based on a priori data. A probabilistic threat exposure map is defined to be the risk of exposure to multiple sources of threat as a function of position. The strategy generates speed and heading angle commands within the dynamic constraints of the UAV. There are three main objectives in order of priority: 1) All of the restricted areas are avoided. 2) The UAV stays within the proximity of the target by a prespecified distance. 3) The total threat exposure level is minimized. During the pursuit, the heading and speed of the target and their time variations are not directly measured but are estimated from the measurements of the target positions. If, for any reason, the sensor can no longer measure the current position of the target, the strategy starts using the predicted target states based on the past measurements to guide the UAV toward the proximity of the target until the UAV detects the target again.

I. Introduction

IN this paper, a target following strategy is introduced for an unmanned aerial vehicle (UAV) flying through an area of multiple sources of threat that are modeled as a probabilistic threat exposure map (PTEM). The PTEM is a map that indicates the threat level of an area due to different types of static threat sources using probability density functions. Recently, there has been an increasing interest in probabilistic approaches in mission planning for the UAVs. This is because the probabilistic approaches are inherently very suitable to handle the uncertainty in the information, such as the locations of the threats. There are several papers in the literature using various probabilistic approaches to deal with the path-planning problem of the UAV applications based on the probabilistic map of the area of operation.[1,2] In Refs. 1 and 2, various path-planning strategies are proposed to minimize the level of threat exposure while flying to a stationary target through an area of multiple threats. This risk of exposure to a source of threat is a function of position, defined to be the probability of becoming disabled by the source of threat at a given position. The probability is assumed to have a Gaussian distribution over the area of operation. The probabilistic threat exposure map is constructed from the probability distribution functions of all of the sources of threat in the area. In Ref. 3, a graph-based probabilistic approach is developed to use the probabilistic map of the area. Unlike the Voronoi graph-based approaches, the nodes and links of the graph are based directly on the probabilistic map. The region of operation is divided into cells whose occupancy value is determined based on the sensor readings. By the application of the conditional probability of occupancy using Bayes rule and the Bellman–Ford algorithm, the shortest path is found.

Because the path-planning strategies rely on probabilistic maps, the construction and online update of the maps are very crucial. In Ref. 4, a probabilistic map of an area with multiple distinguishable moving obstacles is built by using Bayesian estimation, and the Chapman–Kolmogorov equation is used to predict the future movement of obstacles. In Ref. 5, a probabilistic map of an adversarial environment consisting of radars and surface-to-air missiles is constructed. The radar probabilistic map is defined in terms of joint conditional distribution and computed from the data acquired by a noisy sensor. Bayesian rules are used to find the posterior probabilistic map using measurements. In this paper, all radars are assumed to be stationary, and the total number of radars is assumed to be known.

Heretofore, all of the path-planning strategies developed are for a UAV to go to a stationary target position. However, there are some applications in which UAVS are required to follow a moving target. Target following might be in a friendly environment[6] where threat exposure is not a concern. In Ref. 6, a path-planning strategy is developed to track a ground vehicle able to change its heading and vary its speed. The UAV is assumed to track the ground vehicle with an offset vector. When the target following is in a hostile environment, mostly in battle scenarios, reducing threat exposure is as big a concern as tracking the moving target. In this paper, a rule-based intelligent strategy is developed for a UAV to follow a dynamic target while minimizing the level of threat exposure and avoiding restricted areas. The minimization of threat exposure is based on the PTEM, which consists of Gaussian and uniform probability distributions representing various types of threat sources and restricted areas. The UAV is considered to be equipped with a sensor of a limited range that can provide the position of the target for the intelligent strategy. The measurement is modeled to be corrupted by a Gaussian white noise of a mean and variance, but the strategy does not know the nature of the noise. By the use of the measured position of the target, the strategy generates a commanded heading and speed for the UAV so that it can always stay in a proximity circle of a specified radius, which is centered at the target position and moves with the target. In the computation of the commanded signals, the strategy takes into account the dynamic constraints of the UAV such as turning rate and minimum and maximum speeds. As long as the target is within the sensor range, the target position is measured and, based on the measurements, the heading and the speed of the target is estimated. Although the measurement is available, an estimation model for the motion of the target is developed and used to predict the position of the target in the next computation time. When, for some reason, the target is no longer inside the sensor range, the strategy uses the estimation model of the target dynamics to predict the current position, heading, and speed of the target to steer the UAV to reattain the target. If the UAV cannot detect the target in a prescribed time interval, it is assumed to fail to follow the target, and it goes back to its initial position while avoiding the threats.

Presented as Paper 2004-6580 at the AIAA 3rd "Unmanned Unlimited" Technical Conference, Chicago, IL, 20–23 September 2004; received 24 June 2005; revision received 29 July 2005; accepted for publication 5 August 2005.

*Assistant Professor, Department of Mechanical and Aerospace Engineering. Senior Member AIAA.

†Graduate Student, Department of Mechanical and Aerospace Engineering. Student Member AIAA.

The remainder of the paper is organized as follows. The PTEM based on the Gaussian and uniform probability distributions is explained in Sec. II. In Sec. III, we present the intelligent target-following strategy. The model to estimate the target heading and speed from the target position measurements is explained in Sec. IV. Implementation of the target-following strategy in a simulation environment and the results are presented in Sec. V. Finally, the paper is completed with some concluding remarks.

II. PTEM

The PTEM is defined to be the risk of exposure to sources of threat as a function of position. All of the threat sources (exposure to enemy, obstacles, and no-fly zones or restricted areas) are characterized in the same probabilistic framework, that is, the sources of threat are given by their probability distribution functions (PDFs) and the parameters needed in PDFs. For example, if a threat is characterized by a Gaussian PDF, there are two parameters needed to specify fully the threat; the mean value specifies the concentration point (location) of the threat source and the variance specifies how the threat can have an area (or volume for a three-dimensional case) of effectiveness. Gaussian distribution is used to model enemy radars or missiles, whereas uniform distribution is for obstacles or restricted areas in the area of operation. The probability of becoming disabled by a Gaussian threat is characterized by the multidimensional Gaussian law

$$f_{xy,i} = \left\{1 \Big/ \left[2\pi\sqrt{\det(\boldsymbol{K}_i)}\right]\right\} \exp\left[-\tfrac{1}{2}(\boldsymbol{x}-\mu_i)^T \boldsymbol{K}_i^{-1}(\boldsymbol{x}-\mu_i)\right] \quad (1)$$

where

$$\boldsymbol{x} = \begin{bmatrix} x \\ y \end{bmatrix}, \qquad \mu_i = \begin{bmatrix} \mu_{x,i} \\ \mu_{y,i} \end{bmatrix}, \qquad \boldsymbol{K}_i = \begin{bmatrix} \sigma_{x,i}^2 & 0 \\ 0 & \sigma_{y,i}^2 \end{bmatrix}$$

The PDF of the uniformly distributed threat is

$$f_{xy} = \begin{cases} 1/[(b-a)(d-c)], & a \le x \le b, \quad c \le y \le d \\ 0, & (x < a \text{ or } x > b), \\ & (y < c \text{ or } y > d) \end{cases} \quad (2)$$

An example of a PTEM that is used in this paper is shown in Fig. 1. Once the map is constructed, the target-following strategy need not distinguish between the types of threat and needs to use only the probabilistic map for decision making. This is because the map already contains the information about how dangerous the threat sources are to the UAV.

III. Target-Following Strategy

Following a target in an area with multiple threats requires a tradeoff between two possibly conflicting objectives: 1) maintaining the proximity of the target and 2) minimizing the level of threat exposure. The first objective is quantified by the proximity circle, a circle centered at the target position and moving with the target as it moves in the area of operation (Fig. 2). The intelligent following

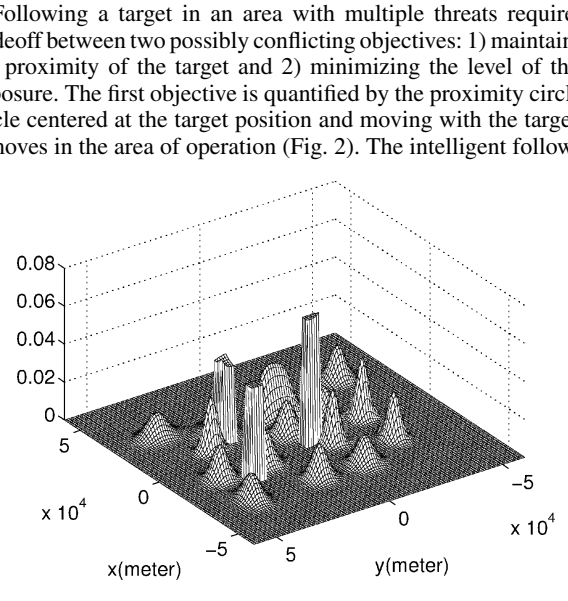

Fig. 1 Probabilistic map of operation area.

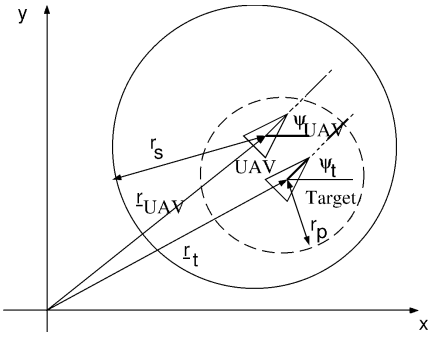

Fig. 2 Proximity and sensor circles.

strategy is to keep the UAV within this circle as long as it is possible. Namely,

$$|\boldsymbol{r}_{\text{UAV}} - \boldsymbol{r}_t| \le r_p \quad (3)$$

where r_p is the radius of the proximity circle and $\boldsymbol{r}_{\text{UAV}}$ and $\boldsymbol{r}_t$ are the position vectors of the UAV and target, respectively. The radius of the proximity circle $\boldsymbol{r}_p$ is a design parameter of the strategy and quantifies how closely the UAV should follow the target.

In this paper, it is assumed that the position of the target is provided for the strategy by an onboard sensor that can only measure the position of the target relative to the UAV. It is also assumed that the target position can always be measured as long as the target is within the sensor range, that is,

$$|\boldsymbol{r}_{\text{UAV}} - \boldsymbol{r}_t| \le r_s \quad (4)$$

where r_s is the sensor range or the radius of the sensor circle as shown in Fig. 2. In other words, the target position is measured during the time when the target is within a circle that is centered at the UAV and moves with it and whose radius r_s is equal to the range of the sensor. However, note that, depending on the type of the sensor, this assumption may not be valid in practice where the sensor has a limited view angle and/or the measurement is obstructed by obstacles such as buildings or terrain.

The radius of the proximity circle r_p determines the level of tradeoff between following the target closely and minimizing the threat exposure level. The bigger the proximity circle, the larger the area where the strategy can search for a trajectory with the lowest probability of becoming disabled. However, as the proximity circle gets bigger, the UAV will follow the target from farther distances. Furthermore, the risk of the target getting outside the sensor range will be greater. Regardless of the size of the proximity circle, the strategy may steer the UAV so far away from the target that the target is no longer in the sensor range. This may happen when the strategy needs to avoid a high threat region or a restricted area. These areas, denoted by A_r, where the UAV should never enter, are quantified by a lower limit $f_{\text{restricted}}$ in the probabilistic map as

$$A_r = \{(x, y) : f_{XY}(x, y) \ge f_{\text{restricted}}\} \quad (5)$$

Another situation that puts the target outside the sensor range occurs when the target suddenly changes its speed or heading. When the target is no longer within the sensor range, the position as well as the heading and speed of the target are estimated by the estimation model developed from the measurement obtained while the target is moving within the sensor circle. The estimation will be utilized to steer the UAV to the target close enough to resume the position measurement. Because the strategy steers the UAV based on the position it will be at the next computation time and not on the current position of the target, when the target is in the sensor range, the estimation model is utilized to compute the current speed and heading of the target to predict the position of the target at the next computation time.

The strategy has three main objectives, which are, in order of priority, as follows:

1) Keep/take the UAV out of A_r.
2) Keep/put the UAV within the proximity circle.
3) Minimize the threat exposure level.

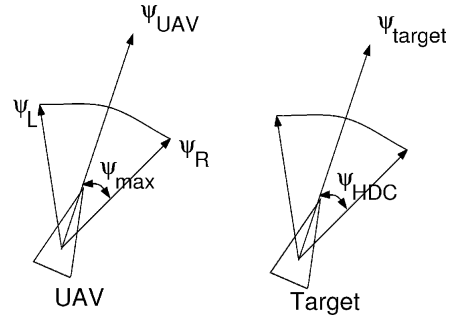

Fig. 3 Heading constraint cone and heading difference cone.

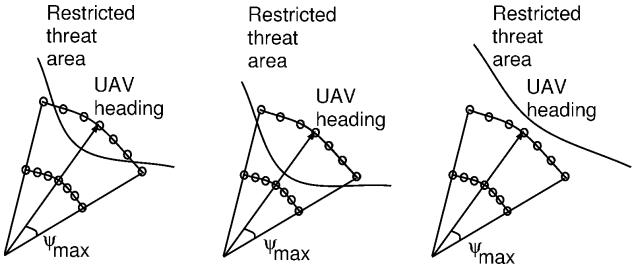

Fig. 4 Searching to avoid restricted high threat region.

To achieve these objectives, the strategy will generate commanded heading ψ_{cmd} and speed V_{cmd} for the UAV. When it does so, it should take into account the dynamic constraints of the UAV, which, in this paper, are as follows:

1) The first constraint is the heading change constraint. The UAV cannot change its heading instantaneously. The rate of heading change is limited due to the dynamics. This is modeled in this paper as a maximum heading constraint $\psi_{\max}$, which is the maximum heading angle change the UAV can make in each simulation step. Here, $\psi_{\max}$ is assumed to be constant regardless of the speed of the UAV, but note that in practice it must be function of speed as well as other states of the UAV. Based on $\psi_{\max}$, a heading constraint cone is defined that moves with the UAV (Fig. 3). It is bounded by ψ_R and ψ_L, where they are defined to be the maximum turning angle to the right and left, respectively. Note that counterclockwise is the positive direction for all of the angles.

2) The second constraints are the minimum and maximum speed constraints. The UAV has flyable minimum $V_{\min}$ and maximum $V_{\max}$ speeds. $V_{\min}$ is chosen to be 10% greater than the stall speed of the UAV. In this paper, the speed constraints are also constant, but in practice they are also functions of the UAV states.

The strategy should not generate any heading or speed command that would violate these constraints. To achieve the objectives without violating the constraints, the strategy uses several rules for the heading and speed difference between the target and the UAV. The strategy evaluates a number of points equally distributed over an arc of a circle bounded by ψ_R and ψ_L to generate heading and speed command in each simulation step. These points are used to evaluate the PTEM to find its minimum value within the constraints of the UAV. The radius of the arc is determined by the current UAV speed and the simulation time step. As the UAV speeds up, the search distance ahead is increased. As the UAV speed decreases, the search is done in a closer distance. The points in this arc are called possible flying points. Moreover, this arc stretches over the permissible heading range. To find out if the UAV is at risk of getting into A_r, instead of searching only next possible flying points the strategy uses a second search arc in which the candidate search points are also distributed with equal intervals, as shown in Fig. 4, which shows how the immediate risk of getting into a restricted area is quantified: 1) If some of the search points on the second arc are outside the restricted area, it is possible to avoid it using one of the search points on the first arc. 2) If all of the points on the second arc are in the restricted area, there is high risk if the sharpest turn is not taken. 3) There is no immediate risk if any of the search points on the first arc are chosen. Search points from the candidates are chosen depending on the dynamic constraints of the UAV and the strategy parameters by means of the intersection areas between cones and circles. In each computation time, the strategy evaluates the PTEM at all of the search points, if there are any, to determine the heading with the lowest probability of becoming disabled. If only some of the points are in the restricted region, the UAV is at low risk of getting into A_r. If all of the points in the second arc are in the restricted region, the UAV is defined to be at high risk of getting into A_r. If none of the points are in the restricted region, then there is no immediate risk of the UAV getting into A_r.

In addition to dynamic constraints, two other mechanisms are also used to keep the UAV in the proximity of the target: 1) keeping the heading difference small and 2) keeping the speed difference small. The first mechanism is quantified by the heading difference constraint ψ_{HDC}, and the second mechanism is quantified by the speed difference constraint.

A. Heading Difference Constraint (HDC)

To keep the heading difference between the UAV and the target small, it should be bounded, which is defined by the HDC angle ψ_{HDC}. This is necessary because the turning radius of a vehicle increases as long as the speed of the vehicle increases. If the heading difference is not bounded, the strategy may change the UAV heading drastically to minimize the threat exposure when the UAV is within the proximity circle. This, in turn, may increase the risk of the target getting outside the proximity circle and eventually outside the sensor range. To restrict the motion of the UAV in and around the direction where the proximity circle is heading, ψ_{HDC} is introduced. Because the correspondence between the vehicle heading and the target heading may be very restrictive in a slow pursuit case, especially if the target stops, a linear relationship is developed between ψ_{HDC} and the estimated target speed V_{est}. There should be a constant HDC ψ^*_{HDC} as long as the V_{est} is greater than a prespecified threshold speed V_{thres}, and starting from V_{thres}, the ψ_{HDC} should go to π as V_{est} goes to zero. Basically, this means that there is no more HDC between the UAV and the target if the V_{est} is zero:

$$\psi_{\text{HDC}} = \begin{cases} \psi^*_{\text{HDC}}, & V_{\text{est}} \geq V_{\text{thres}} \\ \left[\left(\psi^*_{\text{HDC}} - \pi\right)/V_{\text{thres}}\right], & V_{\text{est}} + \pi,\ V_{\text{est}} < V_{\text{thres}} \end{cases} \tag{6}$$

Similar to the heading constraint cone, a heading difference (HD) cone is defined around the target heading moving with the target (Fig. 3),

$$|\psi_{\text{UAV}} - \psi_{\text{target}}| < \psi_{\text{HDC}} \tag{7}$$

The strategy should keep or put the heading of the UAV in the HD cone by commanding the heading angle of the UAV so that the HD between the UAV and the target will be bounded as specified. However, as stated earlier, the UAV cannot change its heading more than $\psi_{\max}$ in a given computation interval. In other words, the heading constraint cone defines the admissible range of heading angles by the UAV, and the HD cone specifies the desired range of heading angles for the UAV.

If there is no overlap between these two cones, as shown in Fig. 5, the closest heading to the target heading, which is obviously the farthest right or left heading of the UAV, will be chosen. As a special case, if there is a 180-deg HD, both the farthest right and left headings will obtain the heading of the UAV at the same proximity to the target heading. Thus, the heading that will provide the least probability of the UAV becoming disabled will be chosen.

The searchable heading range (SHR), as shown in Fig. 6, is defined to be the overlap cone between the heading constraint and HD

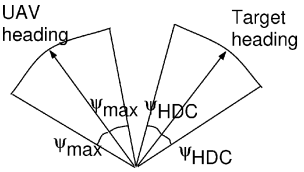

Fig. 5 No overlap between UAV heading and heading difference constraint.

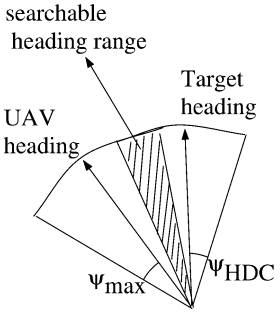

Fig. 6 Overlap between UAV heading and HDC.

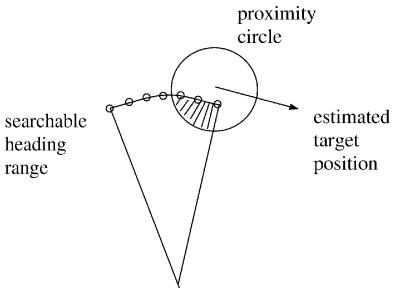

Fig. 7 Searchable points in target proximity range.

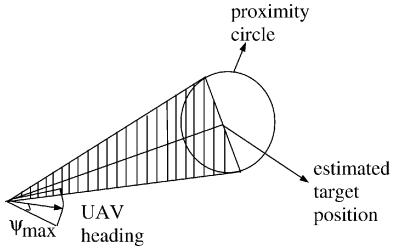

Fig. 8 Steering UAV into proximity circle.

cones. The intersection area between the SHR cone and the proximity circle determines the search points for minimizing the threat exposure (Fig. 7). If this intersection area is empty, it means that the UAV will be outside the proximity circle if the commanded heading is chosen from the SHR cone. To avoid this, the proximity cone (as shown in Fig. 8) is defined to be the set of all of the headings that would take the UAV into the proximity circle from its current position. Because putting the UAV into the proximity circle has a higher priority than minimizing the threat exposure, when the UAV is outside the proximity circle, only the intersection between the proximity cone and heading constraint (HC) cone is investigated. Because the proximity circle is moving with the target, this will also protect the UAV from geting into a limit cycle, which is very objectionable.

B. Speed Difference Constraint

To be able to follow the target, the speed difference between the UAV speed V_{UAV} and the speed of the target V_t should also be bounded, which is defined by

$$|V_{\text{UAV}} - V_t| < V_{\text{DC}} \tag{8}$$

In this paper, speed difference constraint V_{DC} is defined to be zero, which means that the strategy wants the UAV's speed to be equal to the speed of the target as long as the speed of the target is within the UAV's speed constraints. Otherwise, the UAV speed is selected to be $V_{\min}$ or $V_{\max}$.

To achieve the objectives under the given constraints, the strategy uses some rules on the heading and speed difference between the target and the UAV. These rules will vary depending on whether 1) the UAV is at risk of getting into A_r, 2) there is an overlap between HC and HD cones, 3) the UAV is in the proximity circle, and 4) there is an overlap between HC and proximity cones. Depending on the answers (yes/no) to the preceding conditions, there are seven different cases, as shown in Fig. 9.

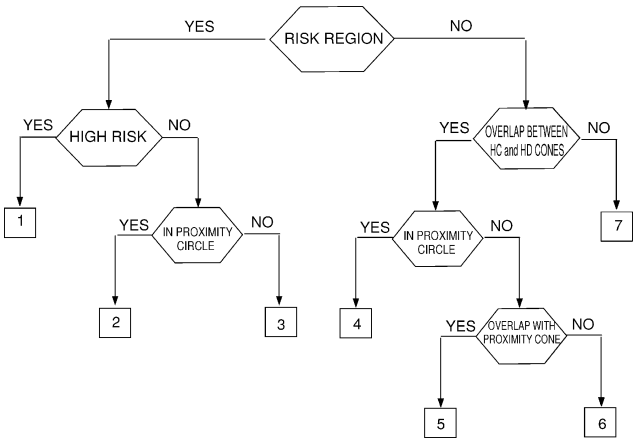

Fig. 9 Decision tree.

In case 1, the UAV is at high risk of getting into A_r. To steer the UAV out of the high risk region as soon as possible, the possible sharpest turn should be taken. To achieve this, the maximum right/left heading is selected without considering ψ_{HDC}, and the commanded speed is selected to be $V_{\min}$ to increase the turning rate of the UAV and to prevent any further incursion:

$$\psi_{\text{cmd}} = \begin{cases} \psi_R, & f_{XY}(X_L, Y_L) \geq f_{XY}(X_R, Y_R) \\ \psi_L, & f_{XY}(X_L, Y_L) < f_{XY}(X_R, Y_R) \end{cases} \tag{9}$$

$$V_{\text{cmd}} = V_{\min} \tag{10}$$

where (X_L, Y_L) and (X_R, Y_R) are the positions corresponding to the left and right headings, respectively.

In case 2, the UAV is at low risk of getting into A_r. To steer the UAV away from the low risk region, the points that are in the restricted region in the second arc of the circle are marked. Corresponding points are eliminated in the first arc of the circle, and then at the remaining points the PTEM is evaluated. If some of these points are in the proximity circle, then the heading with the corresponding search point that will give the lowest probability of becoming disabled $\psi_{\text{min-probability}}$ is chosen and the commanded speed is chosen to be equal to the V_{est} provided as long as it is within the UAV speed constraints,

$$\psi_{\text{cmd}} = \psi_{\text{min-probability}} \tag{11}$$

$$V_{\text{cmd}} = \begin{cases} V_{\min}, & V_{\text{est}} \leq V_{\min} \\ V_{\text{est}}, & V_{\min} < V_{\text{est}} < V_{\max} \\ V_{\max}, & V_{\text{est}} \geq V_{\max} \end{cases} \tag{12}$$

where V_{est} is the estimated speed of the target.

In case 3, none of the points are in the proximity circle. Thus, to get the UAV closer to the predicted target position, the corresponding heading ψ_{closest} that will steer the UAV closest to the predicted target position is chosen. In other words, ψ_{closest} is the corresponding heading of the search point on the first circle of arc with the smallest distance to the predicted position of the target. Moreover, the commanded speed is chosen to be equal to the V_{est} provided that it is within the UAV speed constraints,

$$\psi_{\text{cmd}} = \psi_{\text{closest}} \tag{13}$$

$$V_{\text{cmd}} = \begin{cases} V_{\min}, & V_{\text{est}} \leq V_{\min} \\ V_{\text{est}}, & V_{\min} < V_{\text{est}} < V_{\max} \\ V_{\max}, & V_{\max} \leq V_{\text{est}} \end{cases} \tag{14}$$

In case 4, there is no risk of getting into A_r and there is an overlap between the HC and HD cones, so that the points in the searchable heading range are evaluated. Among the search points in the proximity circle, the corresponding heading that will give the lowest probability of becoming disabled $\psi_{\text{min-probability}}$ is chosen. V_{est} is

also the commanded speed in this case provided that it is within the UAV speed constraints,

$$\psi_{\text{cmd}} = \psi_{\text{min-probability}} \tag{15}$$

$$V_{\text{cmd}} = \begin{cases} V_{\min}, & V_{\text{est}} \le V_{\min} \\ V_{\text{est}}, & V_{\min} < V_{\text{est}} < V_{\max} \\ V_{\max}, & V_{\max} \le V_{\text{est}} \end{cases} \tag{16}$$

In case 5, none of the points in the SHR are in the proximity circle. However, because there is an overlap between SHR and the proximity cone, the UAV heads toward the proximity circle. Thus, to get closer to the target, the heading ψ_{closest} within the HC cone that will move the UAV closest to the predicted target position is chosen. In this case, ψ_{closest} is within the proximity cone. Along the ψ_{closest} direction, the strategy evaluates the PTEM at five more points at every $Vx\delta t$ interval. If the PTEM is less than $f_{\text{restricted}}$ at all of these points, then the strategy will command the speed to increase to put the UAV in the proximity circle as soon as possible. The required velocity V_{req} that will take the UAV into the proximity circle in the next computation is computed. Then, V_{cmd} is computed considering V_{ref} and the speed constraints of the UAV:

$$\psi_{\text{cmd}} = \psi_{\text{closest}} \tag{17}$$

$$V_{\text{cmd}} = \begin{cases} V_{\min}, & V_{\text{req}} \le V_{\min} \\ V_{\text{req}}, & V_{\min} < V_{\text{req}} < V_{\max} \\ V_{\max}, & V_{\max} \le V_{\text{req}} \end{cases} \tag{18}$$

If, at any one of the points, the PTEM is greater than $f_{\text{restricted}}$, then there is a risk of the UAV getting into A_r. To prevent the UAV from approaching A_r, the strategy commands the sharpest turn while the UAV prevents its current speed.

In case 6, there is no overlap between the SHR and the proximity cone. Thus, the UAV heads away from the proximity circle. To turn the UAV toward the proximity circle, the UAV is commanded to turn to ψ_{closest} (which happens to be the sharpest turn in this case) and to match the target speed,

$$\psi_{\text{cmd}} = \psi_{\text{closest}} \tag{19}$$

$$V_{\text{cmd}} = \begin{cases} V_{\min}, & V_{\text{est}} \le V_{\min} \\ V_{\text{est}}, & V_{\min} < V_{\text{est}} < V_{\max} \\ V_{\max}, & V_{\max} \le V_{\text{est}} \end{cases} \tag{20}$$

In case 7, there is no risk of getting into A_r. Additionally, there is not an overlap between the HC cone and the HD cone. Thus, to make the HD between the UAV and the target smaller, the corresponding maximum right/left heading is selected and the commanded speed is selected to be equal to the V_{est}, provided that it is within the UAV speed constraints,

$$\psi_{\text{cmd}} = \begin{cases} \psi_R, & f_{XY}(X_L, Y_L) \ge f_{XY}(X_R, Y_R) \\ \psi_L, & f_{XY}(X_L, Y_L) < f_{XY}(X_R, Y_R) \end{cases} \tag{21}$$

$$V_{\text{cmd}} = \begin{cases} V_{\min}, & V_{\text{est}} \le V_{\min} \\ V_{\text{est}}, & V_{\min} < V_{\text{est}} < V_{\max} \\ V_{\max}, & V_{\max} \le V_{\text{est}} \end{cases} \tag{22}$$

IV. Estimation Strategy

As mentioned before, to make a better decision in following the target, the UAV needs to predict the next position of the target at the current time. Because the UAV is following the target in a threat exposure map, the UAV can also lose the target while avoiding the threats. When that happens, the strategy uses the predicted positions of the target until the UAV catches the target again. In the estimation of the dynamics of the target, the fact that the measurement is noisy should be taken into account and the effect of the noise in the estimation should be minimized. The position of the target is measured in x and y coordinates:

$$\tilde{x} = x + \nu \tag{23}$$

$$\tilde{y} = y + \nu \tag{24}$$

where ν is the zero mean white noise.

Even if the heading and the speed of the target are not measured, the estimation models developed in this paper are for the heading and the speed. The position of the target is computed based on the estimated heading and speed. Because in the estimation algorithm, the measured heading and speed are needed, they are computed from the measured position

$$\tilde{\psi} = \tan^{-1}[(\tilde{y}_2 - \tilde{y}_1)/(\tilde{x}_2 - \tilde{x}_1)] \tag{25}$$

$$\tilde{V} = \sqrt{(\tilde{y}_2 - \tilde{y}_1)^2 + (\tilde{x}_2 - \tilde{x}_1)^2}\Big/\Delta t \tag{26}$$

where $\tilde{\psi}$ and $\tilde{V}$ are considered to be measured values.

Initially, our estimation strategy assumes a batch mode of processing where we use all preceding samples to produce our estimates. More samples means a better estimate. However, the problem with the batch processing is that as more data arrive, calculations will have to be repeated with a larger amount of data, which will result in a computational and memory burden. To resolve this issue, the batch processing is used only until a certain amount of measurement data are obtained. Once a prespecified number of measurements are obtained, then a sequential mode of estimation is initiated. For the sequential estimation, only the preceding estimation and the current measurement are needed.

A second-order estimator is used to estimate the heading and the velocity of the target:

$$\tilde{\psi} = HX + \nu_\psi \tag{27}$$

$$\tilde{V} = HY + \nu_V \tag{28}$$

where

$$X = \begin{bmatrix} a \\ b \\ c \end{bmatrix}, \qquad Y = \begin{bmatrix} d \\ e \\ f \end{bmatrix}, \qquad H = \begin{bmatrix} 1 & t & t^2 \end{bmatrix} \tag{29}$$

Note that because heading and speed measurements are calculated using nonlinear equations, ν_V and ν_ψ are not zero mean white noise. However, in this paper, they are treated as zero mean white noises. To start a linear least-squares estimation, at least three measurements are needed. The equations for the estimation[7] are a batch estimation,

$$\hat{X} = (H^T H)^{-1} H^T \tilde{\psi} \tag{30}$$

$$\hat{Y} = (H^T H)^{-1} H^T \tilde{V} \tag{31}$$

where $\hat{X}$ and $\hat{Y}$ contain the estimated coefficients for the second-order estimator and H is the basis function, and a sequential estimation,

$$\hat{X}_{k+1} = \hat{X}_k + K_{k+1}\left(\tilde{Y}_{k+1} - H_{k+1}\hat{X}_k\right) \tag{32}$$

$$K_{k+1} = P_k H_{k+1}^T \left(H_{k+1} P_k H_{k+1}^T + W_{k+1}^{-1}\right)^{-1} \tag{33}$$

$$P_{k+1} = (I - K_{k+1} H_{k+1}) P_k \tag{34}$$

where K is the Kalman gain matrix that is used to modify the preceding best correction $\hat{X}_k$ by an additional observation to account for the information in the $(k+1)$th measurement subset. P is the covariance update matrix. We start the sequential estimation process by an a priori estimate $\hat{X}_1$ and covariance estimate P_1 that are obtained at the end of the batch processing.

By the use of the batch and sequential processes, heading and velocity estimates of the target are computed by

$$\hat{\psi} = H\hat{X} = \hat{a} + \hat{b}t + \hat{c}t^2 \tag{35}$$

$$\hat{V} = H\hat{Y} = \hat{d} + \hat{e}t + \hat{f}t^2 \tag{36}$$

From the estimated heading and velocity, the predicted position of the target is calculated by

$$x_{\text{predicted}} = x_{\text{preceding}} + \hat{V}\cos\hat{\psi}\,\Delta t \tag{37}$$

$$y_{\text{predicted}} = x_{\text{preceding}} + \hat{V}\sin\hat{\psi}\,\Delta t \tag{38}$$

where the preceding positions $x_{\text{preceding}}$, and $y_{\text{preceding}}$ are from the preceding measured position when measurement was available. If there is no measured position from the preceding computation time, then the preceding estimated position is used.

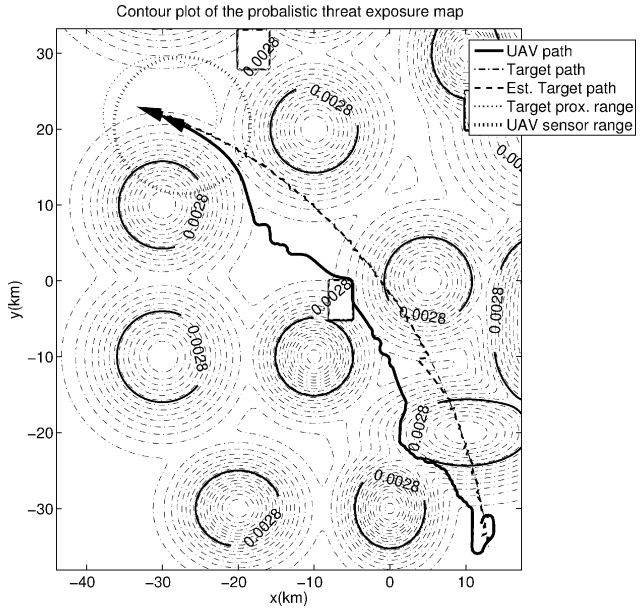

Fig. 10 UAV trajectory generated by strategy to follow target.

V. Implementation of Strategy and Simulation Results

For the implementation of the strategy, five cases are selected in which 17 sources of threat and three no-fly zones are scattered over a 120×120 km area of operation. These cases are selected to show the full capabilities of the algorithm. They cover most of the possible scenarios such as when 1) the UAV starts the pursuit while behind the target, 2) the UAV starts the pursuit while ahead of the target, 3) the target continuously accelerates, 4) the target continuously decelerates and then maintains constant speed that is less than the minimum speed of the UAV, 5) the target stops in a restricted region, and 6) the target stops outside the restricted regions. The probabilistic map of the area is defined and constructed as explained in Sec. II. In all of the simulations, the UAV is considered to have a minimum speed of 180 km/h, a maximum speed of 650 km/h, and a maximum heading angle of 30 deg. The simulation time step is 3 s for all simulations. Strategy design parameters $f_{\text{restricted}}$ and ψ^*_{HDC} are selected to be 0.0028 and 45 deg, respectively. In the trajectories shown later, the UAV trajectory is shown with a solid line, the actual target trajectory is shown with a dash–dot line, and the estimated target trajectory is shown with a dashed line.

Figures 10 and 11 show the first case, in which the target is moving on a third-order trajectory with a linearly increasing speed. The target's initial position, heading, and velocity are $(17, -35)$ km, 97.4 deg, and 392.4 km/h, respectively. The UAV's initial position, heading, and velocity are $(11, -38)$ km, 30 deg, and 288 km/h, respectively. The UAV is assumed to have a 9-km sensor range, and the proximity range is chosen to be 7.5 km. Note from Fig. 10 that the strategy has generated a feasible trajectory for the UAV that follows the target while minimizing the threat exposure and avoiding no-fly zones. Note from Fig. 10 that initially the UAV is ahead of the target. Because the target is behind, the UAV turns around to head toward the target. During the pursuit, the UAV loses the target at 180 s because the target has entered a restricted region. While the UAV flies around the restricted area, the distance to the target gets longer than the sensor range, which prevents the UAV from taking the measurement of the position of the target. Because there is no measurement, the UAV uses the predicted trajectory generated by the estimator to continue the pursuit. Eventually, when the target leaves the restricted region, the UAV is able to fly closer and resume the measurement at 240 s. In the case simulated, because the time interval with no measurement is short and the UAV has obtained enough measurement earlier, the deviation of the predicted trajectory from the actual one is small. Thanks to the satisfactory performance of the estimator, the UAV regains the measurement of

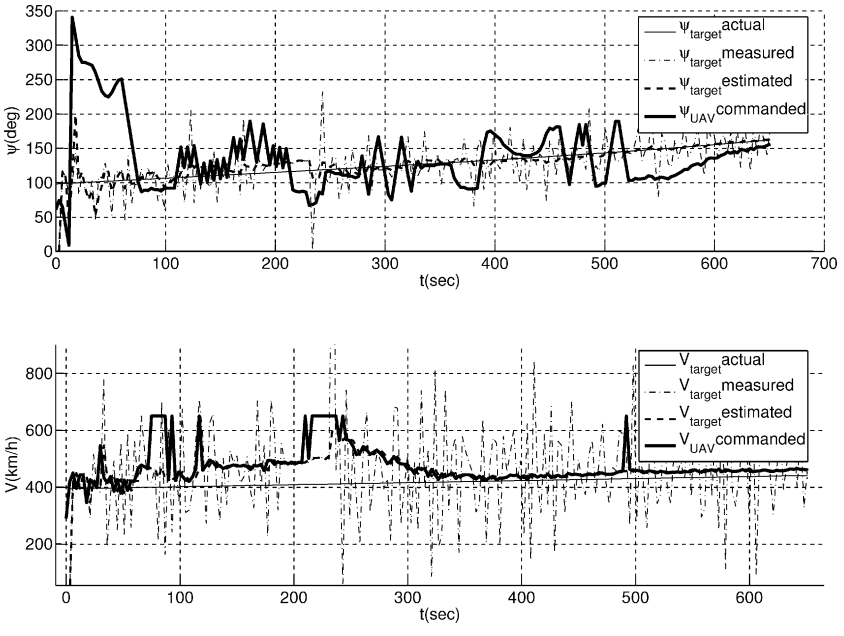

Fig. 11 Actual, measured, and estimated target heading and speed and commanded UAV heading and speed.

the target. Figure 11 shows that during the time when the target is lost and no measurement is taken from 180 to 240 s, the measured signals do not have any noise in them and are exactly the same as the estimated ones. This is because there is, in fact, no measurement, and the last estimated signals are used instead. Note also from Fig. 11 that the commanded UAV speed is always within the constraints and that the UAV matches its speed with the estimated speed of the target as long as the UAV is inside the proximity circle and there are no restricted areas. Nevertheless, because case 5 occurred several times, the UAV speed is commanded to its maximum speed regardless of the estimated target speed. In the simulation, all of the angles are restricted to the range of 0–360 deg. Thus, the commanded heading angle seems to have a jump from 10 to 340 deg at about 15 s. However, this is not a jump but the continuation of the commanded heading change in the clockwise direction while the UAV is turning around toward the target. The sensor noise for the position measurements is Gaussian white noise with a zero mean and standard deviation of 100 m. Because the measured heading and speed are, in fact, computed from the measured positions by using nonlinear equations, their means and standard deviations are different, as can be seen in Fig. 11. Yet, they are assumed to be zero mean white noise in the estimation process.

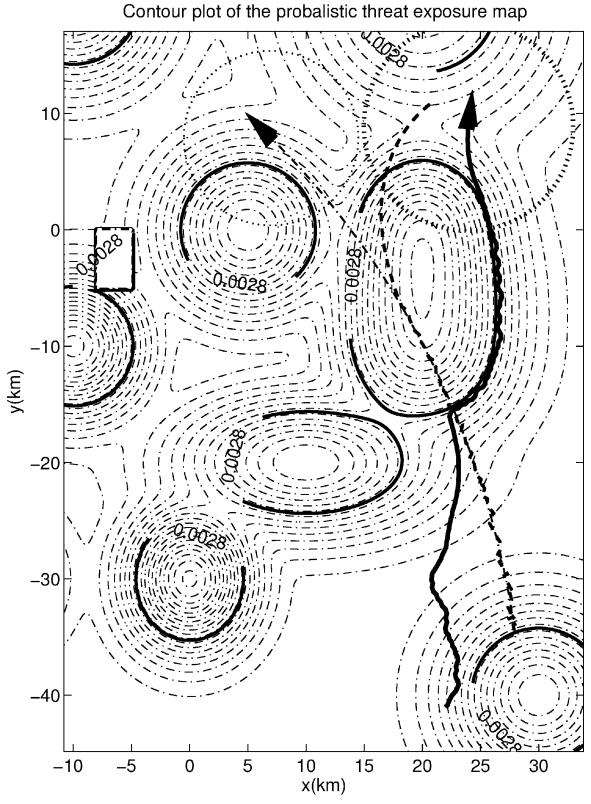

Fig. 12 Insufficient UAV trajectory generated by strategy to follow target: ——, UAV path; –·–, target path; – – –, estimated target path; · · · ·, target proximity range; and ...., UAV sensor range.

The second case, in which the target's initial position, heading, and velocity are (28, −35) km, 97.4 deg, and 392.4 km/h, respectively, is shown in Figs. 12 and 13. The UAV's initial position, heading, and velocity are (22, −41) km, 30 deg, and 288 km/h, respectively. The UAV is assumed to have a 9-km sensor range, and the proximity range is chosen to be 7.5 km. Note from Fig. 12 that the UAV cannot pursue the target. This is because the target passes through a bigger threat region. During the time that the UAV avoids the threat region, the predicted target trajectory significantly diverges from the actual trajectory. Because the UAV follows the predicted trajectory as seen from Fig. 13, it cannot detect the target again. This case shows the limitation of the estimation algorithm. If the target moves unpredictably, letting the target go and stay out of the sensor range for a long time may cause the UAV to lose the target permanently. Nevertheless, as shown in the first case, the incorporation of the estimation algorithm into the following strategy certainly gives the UAV an opportunity to regain the target. This increases the success of the pursuit while avoiding restricted areas and minimizing the threat exposure level.

Figures 14 and 15 show the third case, in which the target's initial position, heading, and velocity are (−15, −35) km, 34.4 deg, and 356.4 km/h, respectively. The UAV's initial position, heading, and velocity are (−11, −30) km, 30 deg, and 288 km/h, respectively. The UAV is assumed to have a 7.5-km sensor range, and the proximity range is chosen to be 5 km. Note from Fig. 14 that because the UAV is initially ahead of the target, the UAV turns around to head toward the target. Furthermore, in this case, the target reduces its speed to 108 km/h in 345 s and maintains that speed in the rest of the pursuit as seen from Fig. 15. Note that the speed of the target is much less than the minimum speed of the UAV during the most of the pursuit. Thus, the UAV reduces its speed to the minimum speed and loiters within the proximity circle when there is no restricted area while minimizing the threat exposure level as shown in Fig. 14.

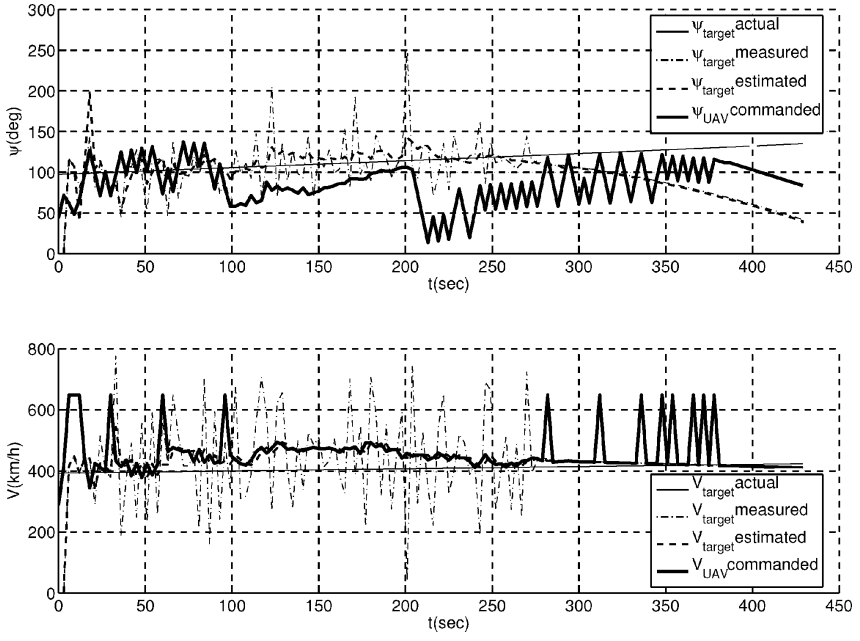

Fig. 13 Actual, measured, and estimated target heading and speed and commanded UAV heading and speed.

Nevertheless, the UAV speed is commanded to its maximum value several times to catch the proximity circle. In all of the time during the pursuit, the commanded speed is within the constraints. Furthermore, there seems to be a jump in the commanded heading angle due to the specified range of angles when the UAV flies with a heading angle close to 0 or 360 deg. Also, there seems to be an amplification in the noise when the target is moving with a heading close to zero. Again, this is due to the conversion of the angles outside the range into their corresponding values in the range, for example 355 deg is the same as −5 deg. This case is presented mainly to show that when the target moves slower than the UAV's minimum speed, the strategy generates a commanded heading to keep the UAV within the proximity circle while minimizing the threat exposure.

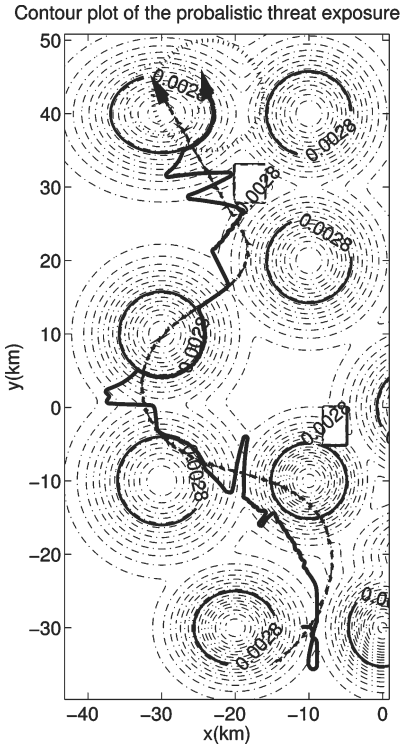

Fig. 14 UAV trajectory generated by strategy to follow slowing target: ——, UAV path; –·–, target path; – – –, estimated target path; · · · · · ·, target proximity range; and ,,,,, UAV sensor range.

The fourth case, in which the target's initial position, heading, and velocity are (−1, −32) km, 57.29 deg, and 356.4 km/h, respectively, is shown in Figs. 16 and 17. The UAV's initial position, heading, and velocity are (5, −30) km, 30 deg, and 288 km/h, respectively. The UAV is assumed to have a 7.5-km sensor range, and the proximity range is chosen to be 5 km. In this case, the target continuously reduces its speed to 0 km/h and stops at 660 s in the middle of a restricted region during the rest of the pursuit as seen from Figs. 16 and 17. In this case, the UAV flies along the boundary of the restricted area when the distance to the target is greater than the radius of the proximity circle. Whenever possible, when the distance from the boundary of the region is smaller than the radius of the proximity circle, as Fig. 17 shows, the UAV tries to minimize the threat exposure while circling around the restricted region. Note from Fig. 17 that the UAV reduces its speed to the minimum speed and maintains it during the rest of the pursuit. However, note that the UAV speed is commanded to its maximum value several times to catch the proximity circle before the target completely stops. Note that, as the target speed get closer to zero, there is an increase in

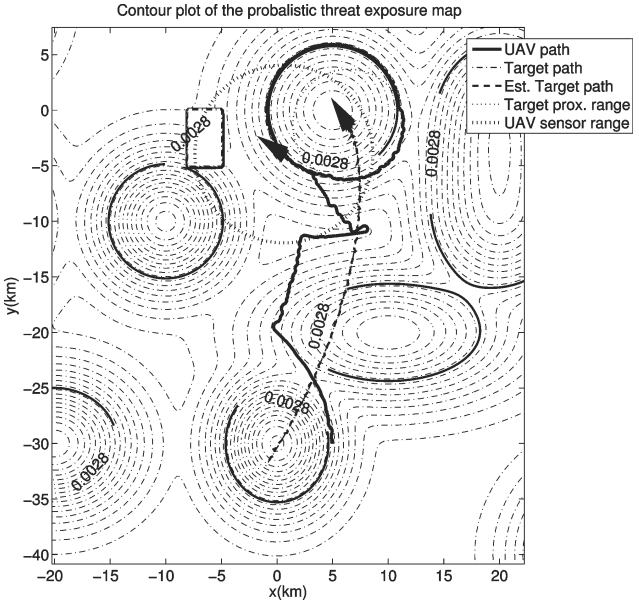

Fig. 16 UAV trajectory generated by strategy to follow slowing and stopping target.

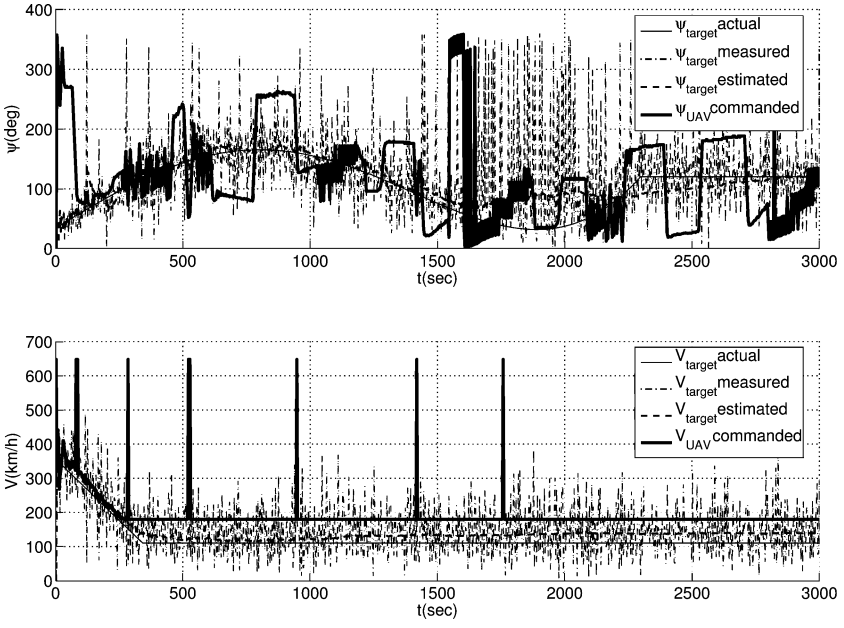

Fig. 15 Actual, measured, and estimated target heading and speed and commanded UAV heading and speed.

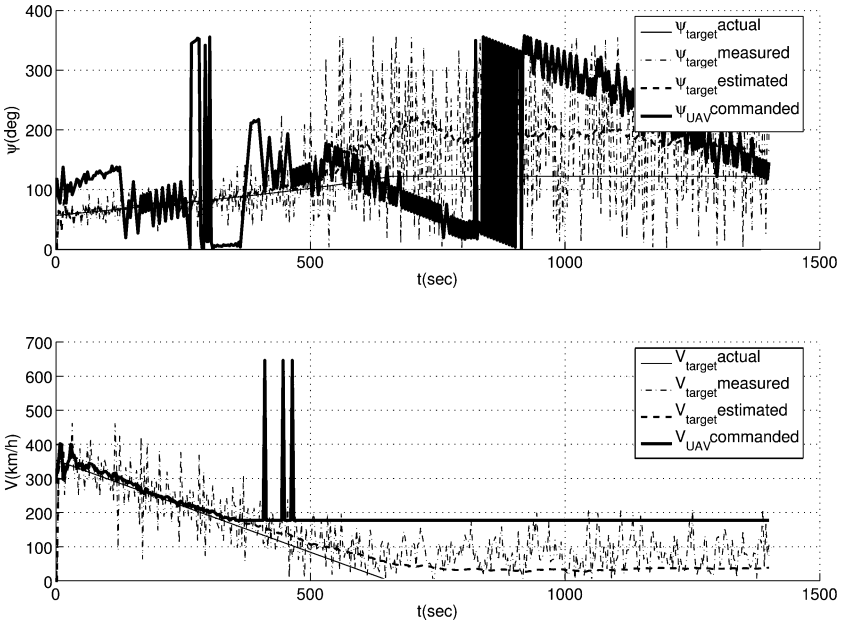

Fig. 17 Actual, measured, and estimated target heading and speed and commanded UAV heading and speed.

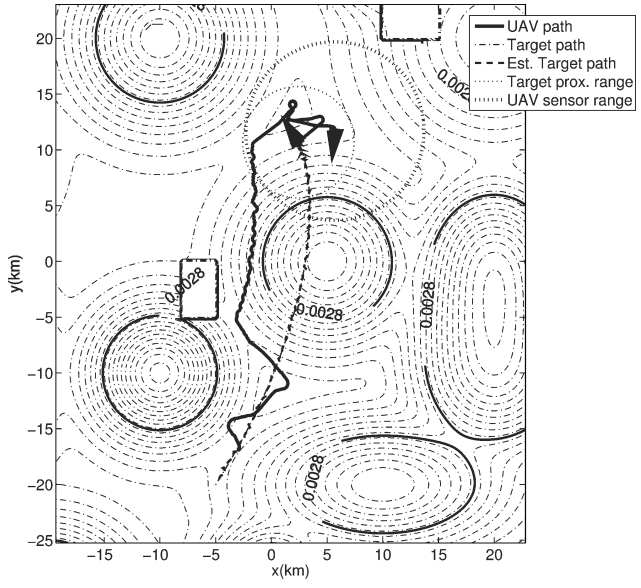

Fig. 18 UAV trajectory generated by strategy to follow slowing and stopping target.

the noise for heading measurements because the target is heading at approximately 90 deg. This basically means that the position change in the x direction is very small, which results in the amplification of the noise. Thus according to Eq. (25), the noise is amplified. Nevertheless, note that when the target stops or moves with a very low speed, the strategy does not take target heading into consideration to command the UAV heading.

Figures 18 and 19 show the fifth case, in which the target's initial position, heading, and velocity are $(-5, -20)$ km, 57.29 deg, and 356.4 km/h, respectively. The UAV's initial position, heading, and velocity are $(-3, -17)$ km, 30 deg, and 288 km/h, respectively. The UAV is assumed to have a 7.5-km sensor range, and the proximity range is chosen to be 5 km. In this case, the target constantly reduces its speed, and at 660 s it stops in a region where there are no restricted areas during the rest of the pursuit as seen from Figs. 18 and 19. In this case, the UAV loiters inside the proximity circle while minimizing the threat exposure. The UAV speed is commanded to its minimum value and maintains it during the pursuit as seen from Fig. 19. Because of the same reasons discussed earlier, there is an increase in the noise for heading measurements.

Table 1 Effects of proximity range to total UAV trajectory length and threat exposure

	UAV	
r_{prox}, km	L_{traj}, km	Probability
0.5	91.177	0.0755
3.0	86.964	0.0459
5.0	85.702	0.0340
7.5	84.987	0.0307
8.0	84.721	0.0291

In all cases, it is shown that threats and no-fly zones are avoided perfectly, yet the UAV may violate these regions for a very short time while trying to avoid them. This does not mean that the UAV has failed because $f_{\text{restricted}}$ is a parameter of the strategy, and it is specified with a safety margin that will protect the UAV from violating the real restricted areas. The reason behind flying very close to restricted areas is that the UAV is trying to be in the proximity circle all of the time, which means that it is trying to compromise between safer and closer trajectories to the target. Thus, as the proximity circle gets bigger, the total probability of the UAV becoming disabled will decrease, which means that the UAV will have a chance to follow a much safer trajectory. However, if the proximity radius is greater than the sensor range, then the UAV will very likely lose the target. The effects of the parameters of the strategy on the total length and total probability of the UAV are given in tabular forms in the remainder of this section, which are obtained from the first case where the target is continuously accelerating. In this case, the total length of the target trajectory is 75.216 km and the total probability of becoming disabled is 0.1273.

Table 1 shows that as the proximity range increases, the total probability of the UAV becoming disabled decreases, and the total length of the UAV decreases accordingly. Increasing the proximity range will give the strategy more flexibility to minimize the map while it is inside the proximity circle. Furthermore, as long as the UAV stays in the proximity circle, it will make fewer maneuvers to get closer to the target, which means that a safer and a shorter trajectory will be followed. As the ratio of the sensor to proximity ranges approaches 1, following the target may become harder. Once $r_{\text{proximity}}$ becomes greater than the r_{sensor}, the target will be more likely

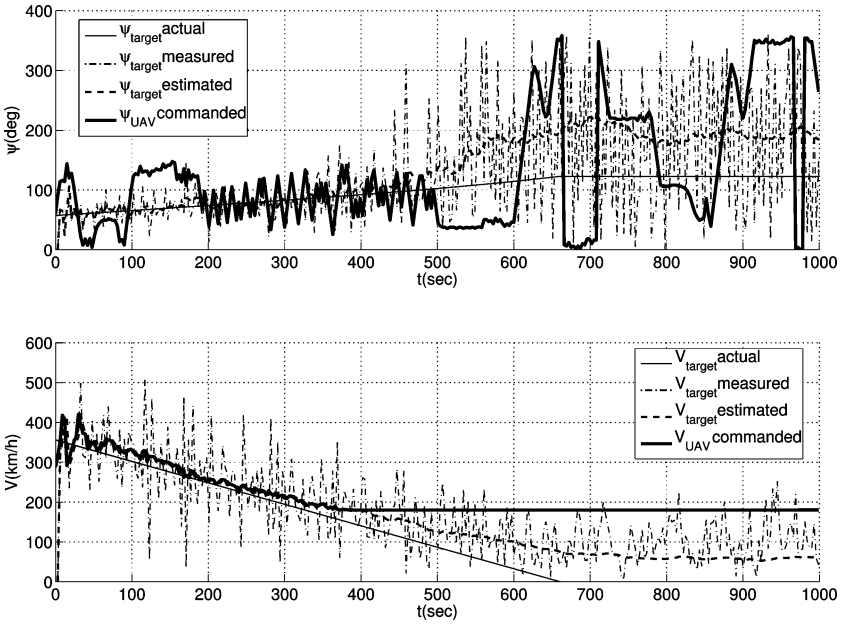

Fig. 19 Actual, measured, and estimated target heading and speed and commanded UAV heading and speed.

Table 2 Effects of heading difference constraint ψ^*_{HDC} to total UAV trajectory length and threat exposure

	UAV	
ψ^*_{HDC}, rad	L_{traj}, km	Probability
$\pi/4$	84.987	0.0307
$\pi/6$	81.906	0.0326
$\pi/12$	81.906	0.0688
$\pi/18$	81.906	0.0689
$\pi/36$	81.906	0.0694

Table 3 Effects of $f_{\text{restricted}}$ to total UAV trajectory length and threat exposure

	UAV	
f_{restrict}	L_{traj}, km	Probability
0.0028	84.987	0.0303
0.0050	83.834	0.0454
0.0075	83.538	0.0529
0.0100	83.217	0.0535
0.0200	83.217	0.0535
0.1000	83.217	0.0535
0.5000	83.217	0.0535
1.0000	83.217	0.0535

to be outside the sensor range. In this case, if the estimator is not good enough to follow the target trajectory, the UAV cannot catch the target again and, thus, the amount of measurements about the target movement might not be adequate to develop a good estimation model. Note that in all of the cases, the probability of the UAV becoming disabled is much less than that if it would follow exactly the trajectory of the target.

Note from Table 2 that if the HDC constant ψ^*_{HDC} is decreased, the probability of the UAV becoming disabled will increase because there will be fewer points in the searchable area, and the UAV will not be allowed to turn its heading to the points that will minimize its threat exposure more. However, this parameter does not affect the total length significantly. Note that, if the ψ^*_{HDC} is specified larger than $\pi/4$, the UAV would lose the target permanently. Thus, even if the threat exposure level is reduced as ψ^*_{HDC} is increased, the HD should be restricted, especially during high-speed pursuits.

Table 3 shows the effect of $f_{\text{restricted}}$ on the probability of becoming disabled and the total length of the trajectory. As $f_{\text{restricted}}$ is increased, the probability of the UAV becoming disabled will increase because it will have permission to enter higher threat regions. However, note that when $f_{\text{restricted}}$ is greater than 0.01, any further increase in $f_{\text{restricted}}$ does not affect the UAV motion, and, thus, the probability and the length stay the same. This can be explained by the fact that, even if there is no restricted area, the strategy still minimizes the threat exposure map as long as it stays in the proximity range of the target. Note that even this maximum probability of the UAV becoming disabled is much less than the probability of becoming disabled if the target's trajectory was followed exactly. Note also that this maximum probability can be further decreased by varying the other parameters of the strategy, such as increasing the proximity range.

VI. Conclusions

A new target following strategy is developed for UAVs pursuing a moving target while flying in an area of multiple threat sources. The strategy generates heading and speed commands within the dynamic constraints of the UAV to follow the target while avoiding restricted regions and minimizing threat exposure. During the pursuit, the position of the target is measured only when the target is within the sensor range. The speed and heading of the target are estimated based on the noisy measurement data by a second-order linear least-square estimator with a batch and sequential mode of processing.

The strategy is implemented in a MATLAB®-based environment and simulated for several cases to show the effectiveness of the strategy. The simulation results have shown that the dynamic target pursuit can be succesfully achieved in almost all possible pursuit scenarios. However, when the target stays beyond the sensor range for a long time, the UAV may lose the target permanently due to the limitation of the estimation algorithm. Nevertheless, as shown in most of the cases, the incorporation of the estimation algorithm into the pursuit strategy certainly gives the UAV an opportunity to regain the target. This increases the success of the pursuit and survivability by enabling the UAV to get away from the target to avoid restricted areas and to minimize threat exposure level.

Furthermore, the performance of the pursuit strategy can be improved via variation of the strategy parameters such as maximum allowable threat exposure level, specified proximity distance to the target, and the allowable heading angle difference between the target and the UAV. The variation of the parameters can be used to quantify

the tradeoff between following the target closer and following the target with a lower threat exposure level.

References

[1]Dogan, A., "Probabilistic Approach in Path Planning for UAVs," Inst. of Electrical and Electronics Engineers, Paper 7929467, Oct. 2003.

[2]Dogan, A., "Probabilistic Path Planning for UAVs," AIAA Paper 2003-6552, Sept. 2003.

[3]Butenko, S., Murphey, R., and Pardalos, P. M., *Cooperative Control: Models, Applications and Algorithms*, Kluwer Academic, Dordrecht, The Netherlands, 2003, pp. 95–111.

[4]Jun, M., and D'Andrea, R., "Probability Map Building of Uncertain Dynamic Environments with Indistinguishable Obstacles," *Proceedings of the American Control Conference*, Inst. of Electrical and Electronics Engineers, 2003, pp. 3417–3421.

[5]Hespanha, J. P., Kizilocak, H., and Ateskan, Y. S., "Probabilistic Map Building for Aircraft-Tracking Radars," *Proceedings of the American Control Conference*, Vol. 6, Inst. of Electrical and Electronics Engineers, 2001, pp. 4381–4386.

[6]Sengupta, R., Lee, J., Huang, R., Vaughn, A., Xiao, X., Hedrick, J. K., and Zennaro, M., "Strategies of Path Planning for a UAV to Track a Ground Vehicle," Proceedings of the Second Annual Symposium on Autonomous Intelligent Networks and Systems, IEEE Control Systems Society and Office of Naval Research, June–July 2003.

[7]Bar-Shalom, Y., Li, X., and Kirubarajan, T., *Estimation with Applications to Tracking and Navigation*, Wiley, New York, 2001, pp. 145–161.